Monte Carlo dosimetry of the most commonly used ^{192}Ir high dose rate brachytherapy sources

JF Almansa López[1], J Torres Donaire[2*], R Guerrero Alcalde[3]

[1]Servicio de Física y Protección Radiológica. Hospital Universitario Virgen de las Nieves. Granada.
[2]Servicio de Radiofísica y Protección Radiológica. Hospital General Universitario de Ciudad Real.
[3]Servicio de Radiofísica. Hospital Universitario San Cecilio. Granada.

Received: 25/03/2011 - Accepted: 26/11/2011

The ^{192}Ir sources are the most commonly used in brachytherapy treatments of high dose rate. The aim of this paper is to provide the characteristic functions established by AAPM Task Group 43 (TG-43) using PENELOPE 2008.1 simulation code for the most widespread ^{192}Ir sources in Spain: Gammamed Plus and Varisource 2000 sources distributed by Varian Medical Systems and MicroSelectron source distributed by Nucletron BV. Also the new model, mHDR-v2r, has been characterized for MicroSelectron source, including some changes from previous design, mHDR-v2.

Radial dose function, anisotropy function, air-kerma strength, dose rate constant and absorbed dose rate in water tables are in good agreement with available data from other calculations. The obtained values for the dose rate constant have been 1.111±0,002 cGy/(hU) for Gammamed Plus source, 1.111±0.002 cGy/(hU) for MicroSelectron mHDR-v2 source, 1.112±0.002 cGy/(hU) for MicroSelectron mHDR-v2r source and 1.096±0.002 cGy/(hU) for Varisource 2000 source. Complete dosimetric results are available in http://bqseeds.sarh.es.

In this work, results have been obtained for the studied sources with the same calculation conditions and simulations that meet current recommendations.

Key words: Monte Carlo dosimetry, ^{192}Ir, HDR, TG-43, PENELOPE.

Introduction

^{192}Ir high dose rate sources are widely used in brachytherapy applications by inserting needles and catheters or implants that allow the source to reach tumor lesions in different anatomical locations: uterus, cervix, prostate, breast, esophagus, bronchi and others. The dosimetric characterization of these sources and seeds is fundamental for the brachytherapy treatment planning. Monte Carlo (MC) calculations allow us to achieve this goal by modelling the geometry of the radioactive source and the processes of interaction of the particles emitted in the decay process. It also allows us to obtain data even at points where the performance of an experimental measurement is very difficult.

The AAPM TG-43[1] establishes how to characterize dosimetry of brachytherapy sources. The update of this protocol (TG-43 U1)[2] for low energy sources for interstitial brachytherapy (less than 50 keV average energy) includes recommendations for the implementation of dosimetry calculations through MC simulations that are also applicable to higher energy sources (definition of the radial extension of the results, simulation of enough number of histories for ensure a good statistical uncertainty, recommendation of certain cross sections libraries,...). Besides, Li et al[3] present recommendations for sources that emit photons with energies above 50 keV following the TG-43 U1. This paper suggests following the scheme of TG-43 U1 and recommends that the calculation uncertainties for absorbed dose rate tables should remain below 6% at 2σ and spatial resolution must be less than 2 mm, but does not include recommendations regarding the spatial extent of the calculation.

In this work, MC simulations have been performed for the dosimetry characterization of Gammamed Plus and VS2000 VariSource, distributed by Varian Medical Systems, and MicroSelectron (mHDR-v2 model), distributed by Nucletron BV, ^{192}Ir high dose rate brachytherapy sources. The characteristic TG-43 functions and parameters have been obtained incorporating the recommendations given in TG-43 U1, as well as those suggested by Li et al[3]. Thus, the results have been achieved up to a radial extension of 40 cm with a statistical uncertainty less than 2% for a coverage factor $k = 1$.

For MicroSelectron source, MC dosimetry has been also performed for the new model source, mHDR-v2r, incorporating the changes introduced by the manufacturer.

* Correspondence
Email: javitorresdonaire@yahoo.es

All MC calculations were performed with the same methodology and identical simulation conditions (materials modelled with the same composition, same calculation grid for the energy deposition, same simulation code and parameters,...) which improve the intercomparison of results between different sources.

Material and methods

Sources and radionuclides description

MicroSelectron mHDR-v2 (MS-v2) source have been modelled following the work of Daskalov et al[4]. The source is composed of a cylindrical core of 3.6 mm length and 0.65 mm diameter whose extremes are truncated cones of 0.25 mm height and major and minor diameters of 0.65 mm and 0.5 mm, respectively. The source capsule is made of AISI 316L stainless steel with 4.5 mm total length, 0.9 mm diameter and a hemispherical termination. The connection to the cable responsible for the source movement is through a truncated cone for adapting the different diameters. This cable is modelled as a cylinder with 0.7 mm diameter of AISI 314 stainless steel with density of 4.81 g/cm^3 to account for the interlace responsible for its flexibility.

The new model MicroSelectron mHDR-v2r (MS-v2r) source has been made following the work of Granero et al[5]. The most remarkable changes over the previous model affect the active core of the source, now modelled as an iridium cylindrical core of 0.6 mm diameter and 3.5 mm length. Besides, the union of the source to cable has been modified.

GammaMed Plus (GM) source has been modelled following the work of Ballester et al[6], but the end of the source has been modelled with a truncated cone according to the information provided by the manufacturer. Thus, the core is modelled as an iridium cylinder of 3.5 mm length and 0.6 mm encapsulated with AISI 316L stainless steel with internal diameter of 0.7 mm, external diameter of 0.9 mm and maximum length of 4.5 mm to form a cylinder with truncated cone end. Encapsulation is directly connected to a cable that has been modelled as a cylinder of an AISI 304 stainless steel of 5.6 g/cm^3 density and of 0.9 mm diameter.

VariSource VS2000 (VS) source has been modelled through Angelopoulos et al[7] work. The source active core is composed of two cylinders with hemispherical end of 2.5 mm length and 0.34 mm diameter and it's made of iridium. This core is encapsulated at the end of a cylindrical guide of 150 mm length and 0.59 mm diameter that have a hemispherical end composed of a nickel and titanium alloy. The distance between the end of the capsule and the end of the core is of 1 mm.

Every model details are shown in fig. 1 with materials used in its simulation and dimensions expressed in mm. Changes between the new model MicroSelectron mHDR-v2r and mHDR-v2 are also shown. The composition of the materials for the simulations is described in table 1. Stainless steel data have been averaged from standards for this alloys[8]. Water and air compositions are collected from TG-43 U1.

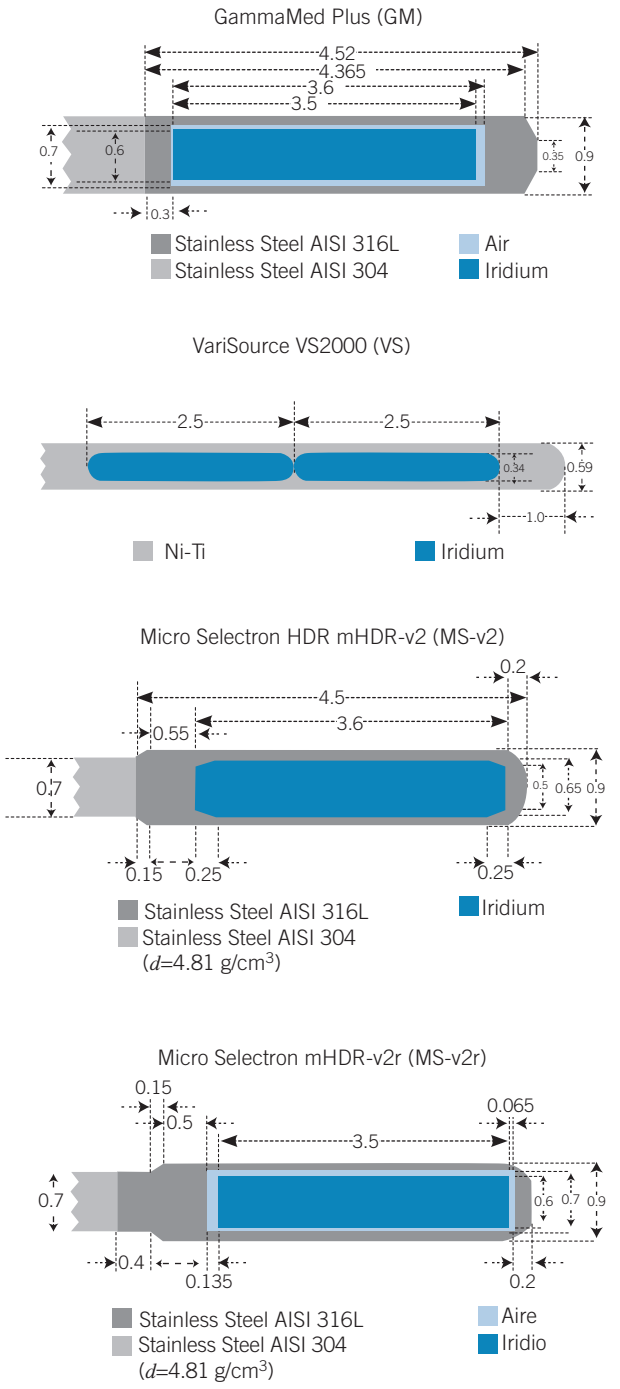

Fig. 1. Source geometries. Dimensions are in millimetres.

Table 1. Fractions by weight of each material in simulations.

Material composition	Iridium	Ni-Ti	AISI 316L	AISI 304	Water	Air
H	---	---	---	---	11.1	0.073
C	---	---	0.03	0.08	---	0.012
N	---	---	0.1	0.1	---	75.033
O	---	---	---	---	88.9	23.608
Si	---	---	0.75	0.75	---	---
P	---	---	0.045	0.045	---	---
S	---	---	0.03	0.03	---	---
Ar	---	---	---	---	---	1.274
Ti	---	44.25	---	---	---	---
Cr	---	---	17	19	---	---
Mn	---	---	2	2	---	---
Fe	---	---	65.545	68.745	---	---
Ni	---	55.75	12	9.25	---	---
Mo	---	---	2.5	---	---	---
Ir	100	---	---	---	---	---
Density (g/cm^3)	22.42	6.5	8.03	5.6 (GM cable) 4.81 (MS cable)	0.998	1.20x10^{-3}

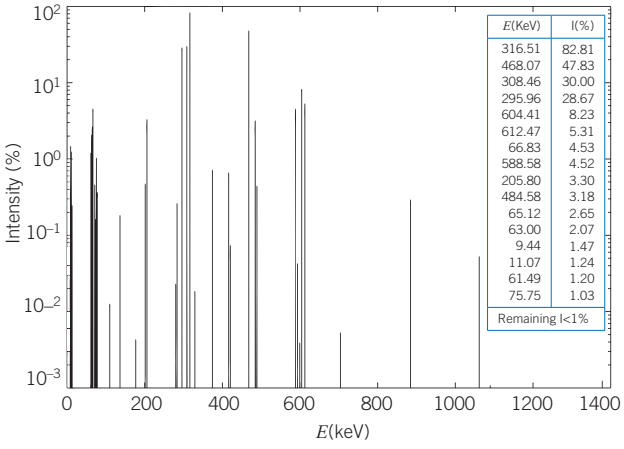

Fig. 2. Photon energy spectrum emitted by ^{92}Ir disintegration. Lines with major contribution (more than 1 photon by 100 disintegrations) are included in the inserted table.

In all cases, it is considered that the ^{192}Ir radionuclide is uniformly distributed in the iridium core.

^{192}Ir is a product of the metallic iridium neutron bombardment with a half life of 73.831(8) days* that decay through beta emission (95.24(4)% probability) and electron capture (4.76(4)% probability). The emission spectrum of characteristic X-rays emission and desexcitation products is shown in fig. 2. A number of 2.3575 photons by disintegration have been considered. These values have been obtained from LUND/LBNL[9] nuclear database. Electrons from beta decay have not been simulated, being their contribution lower than the estimated uncertainty in defining the geometry, ^{192}Ir distribution in the source or the uncertainty of the cross sections used by simulation codes[10].

* The value in parentheses indicates the uncertainty on the last significant figure, read 73.831(8) as 73.831 ± 0.008.

Simulation code

PENELOPE[11] is a general purpose MC code that allows us to simulate the transport of electrons and photons of energies ranging from a few hundred eV to 1 GeV in a wide variety of materials. In addition, PENELOPE allows describing particle transport in complex geometries and provides an excellent description of electron transport at low energies. Photon interactions described in the code are: Rayleigh scattering, photoelectric absorption, Compton scattering and pair production. The Rayleigh scattering is based on the Born approximation with non-relativistic form factors[12,13]. In the case of photoelectric absorption, PENELOPE gets their tables from the EPDL[14] ("Evaluated Photons Data Library") library of cross sections. Compton scattering is

described by relativistic impulse approximation which takes into account the Doppler broadening effect, which is not considered in the library of cross sections in the program EPDL97 nor XCOM[16]. Pair production is not in the energy range of the simulations of this paper, E <600 keV. These characteristics make of PENELOPE a useful tool for applications in medical physics.

In this work PENELOPE version 2008.1 has been used.

Air-kerma strength (S_k)

For the specification of brachytherapy sources, TG-43 defines air-kerma strength, S_k, as the air kerma rate in free space at a distance d multiplied by the square of the distance, d^2.

$$S_k = K(d)d^2 \tag{1}$$

In addition, to determine S_k for line sources, the TG-43 protocol recommends to set a distance d of 1 m in the perpendicular direction to the axis of the source, $\theta=\pi/2$.

In this paper, air kerma rate has been calculated as a function of polar angle, θ, and the distance to the source, d, according to[17]:

$$K(d,\theta) = \int \phi_E(\theta) E \frac{\mu_{tr}}{\rho}(E)\,dE \tag{2}$$

where d and θ are the polar coordinates of the point where air kerma rate is computed, $\phi_E(\theta)$ is the photon fluence rate with energy E for the angle θ, E is the photon energy an $\mu_{tr}(E)/\rho$ is the mass energy-absorption coefficient for the medium (air).

In the energy range of ^{192}Ir sources and for the materials considered, the energy loss fraction through radiative processes for charged particles, g, is negligible so the mass energy-absorption coefficient can be approximated by the mass absorption coefficient:

$$\frac{\mu_{en}}{\rho} = \frac{\mu_{tr}}{\rho}(1-g) \cong \frac{\mu_{tr}}{\rho} \tag{3}$$

The mass energy-absorption coefficients for air have been obtained by interpolation of the data published by the NIST[19]. A segmental cubic spline fit has been used for interpolation.

The photon fluence has been determined by MC simulations considering the source immersed in vacuum and accumulating the photons passing through a spherical surface of 1 m radius centered on the active core as function of its energy and polar angle. The binning for the surface has been $\Delta\theta=1°$. The detected photon energy has been accumulated in bins of $\Delta E=1$ keV to avoid artefacts due to the use of greater width cells[10]. All the simulation parameters have been fixed at values equal for all materials, except DSMAX value: C1 = 0.05, C2 = 0.05, WCC = 10^4 eV, WCR = 10^3 eV. The selected absorption energies were: 10^9 eV for electron EABS and 5×10^3 eV for photons EABS. For the DSMAX parameter, the selected values were 0.006 cm for iridium, 0.0005 cm for air, 0.001 cm for capsule and 0.009 cm for the cable. The simulated histories number was 6.4×10^{10} for all sources.

Under these conditions the air kerma rate in free space has been calculated using the expression:

$$K(d,\theta) = \sum_{E_i} \phi_{E_i}(\theta) E_i \frac{\mu_{en}}{\rho}(E_i)\Delta E \tag{4}$$

where E_i is the central value of each bin in the energy histogram of width ΔE.

Two sets of kerma MC simulations have been performed to study the influence of the low energy photon spectrum ($E<14$ keV) and characteristic X-rays of the iridium L shell ($E=13.4$ keV). One of the simulations includes these values in simulations and the other avoids low energy photons in the simulation using photon energy absorption values of 20 keV for the iridium and 5 keV for the capsule.

Absorbed dose rate in water

To calculate the absorbed dose rate in water, the source is immersed in a semi-infinite water phantom ($\rho=0.998$ g/cm^3, radius=1 m) with the center of the coordinate system in the center of the iridium core and the Z axis along the source and the positive sense towards the end of the capsule.

In order to make some comparisons with other published data that do not share these calculation conditions, simulations have been performed in a finite phantom of 15 cm radius and using a value of 1 g/cm^3 for the water density.

The number of simulated histories has been of 1.575×10^{10} for GammaMed Plus source, 1.05×10^{10} for MicroSelectron mHDR-v2 and MicroSelectron mHDR-v2r sources and 0.96×10^{10} for VariSource 2000 source. The deposited energy in each interaction of the transport of electrons and photons simulation has been accumulated to perform the calculation, so absorbed dose rate per S_k unit in the accumulation volume has been obtained. We have used two different spatial discretizations: One with annular cylindrical cells of Δz = 0.05 cm and Δr = 0.05 cm and other with spherical coordinates discretization cells of $\Delta r=0.05$ cm and $\Delta\theta=1°$.

The simulation parameters used for dose rate in water are the same as for the kerma calculation, except for absorption energy: 10^5 eV for electron EABS and 10^3 eV for photon EABS. A value of 10^{35} cm has been chosen for DSMAX parameter in water. This value ensures that electrons with energy below EABS have a range lower than a half of any dimension of the energy storage cells, according to the PENELOPE[11] manual, for the continuous slowing down approximation.

A 2D table for absorbed dose rate in water has been made through obtained calculations and the dose rate constant, dose radial function and anisotropy function have been calculated following the AAPM TG-43 protocol for the linear source approximation. The considered active length for each source model has been 3.5 mm for the source GammaMed Plus, 3.6 mm MicroSelectron mHDR-v2 source, 3.5 mm MicroSelectron mHDR-v2r source and 5 mm for VariSource 2000 source.

Compilations and other references

The obtained data have been compared with collected data of dosimetric parameters of brachytherapy sources that are available in http://www.physics.carleton.ca/clrp/seed_database[20] (dataset from Taylor et al[21] that with homogeneous calculations using EGSnrc code simulations) and in http://www.uv.es/braphyqs[22] (compilation of results from various authors and where the simulation characteristics, such as phantom size or simulation code, depend on the reference).

Also, comparisons have been made with previous PENELOPE based results by Berenguer et al[23] and Casado et al[24], and recent results of Granero et al[5] for MS-v2r source available in ftp://ftp.aip.org/epaps/medical_phys/E-MPHYA6-38-055101.

Uncertainties

The uncertainty associated with the results is due to statistical noise of the simulations, evaluated following the methodology described by Salvat et al[11]. One standard deviation has been shown as the uncertainty. We used the quadratic propagation of uncertainties in the calculation of uncertainty for magnitudes calculated from the simulations: absorbed dose rate constant, radial dose function and anisotropy function. These uncertainties are called type A[25].

Type B uncertainties have not been included in this analysis. A detailed discussion for their estimation in the field of brachytherapy sources and the difficulties associated with this question can be found in TG-43 U1 and AAPM TG-138[26] report.

Results and discussion

Air kerma rate

"Air-kerma strength" (S_k) per unit of source activity at the TG-43 reference point (d=1 m, θ=90º) obtained for the different sources has been:

- **GammaMed Plus:** $9.87(2)\times10^{-8}$ U/Bq.
- **VariSource 2000:** $10.32(2)\times10^{-8}$ U/Bq. This value is in good agreement with that obtained by Casado et al[24], $10.15(21)\times10^{-8}$ U/Bq, and Angelopoulos et al[7], $10.27(5)\times10^{-8}$ U/Bq.
- **MicroSelectron mHDR-v2:** $9.78(2)\times10^{-8}$ U/Bq. This value is in good agreement with that obtained by Berenguer et al[23], $9.82(3)\times10^{-8}$ U/Bq.
- **MicroSelectron mHDR-v2r:** $9.86(2)\times10^{-8}$ U/Bq. This value differs 0.8% from the value obtained for the model mHDR-v2.

Air kerma rate depending on polar angle at 1 m is shown in fig. 3 for the analysed sources. A significant dependence on it can be observed.

The influence of low energy photons in S_k has been studied, following the work of Borg et al[10]. MC simulations have been performed taking and not taking into account these low energy photons. Our results show that not taking into account the lower energy photons at 20 keV in energy iridium and less than 5 keV in the steel capsule leads to a reduction of 0.01%. On the other hand, the inclusion of low energy photons does not carry a significant cost in simulation computer time.

Absorbed dose rate tables (along-away dose tables)

The achieved statistical uncertainty is kept below 2% throughout the considered space, except in the longitudinal axis, due to the small size of accumulation

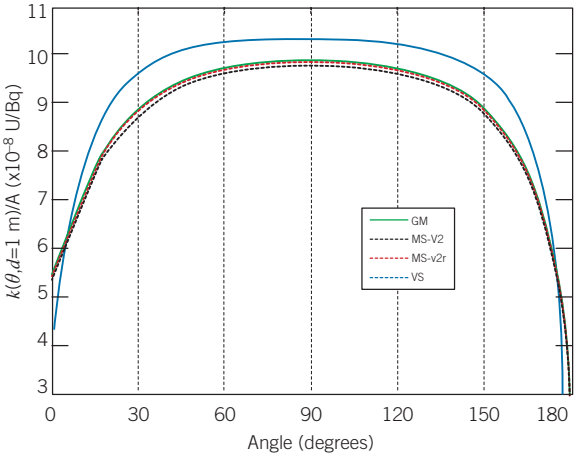

Fig. 3. Air kerma rate at 1 m per activity unit as a polar function, $K(\theta, d = 1m)/A$.

Table 2. Comparison of absorbed dose rate constants in cGy/(hU).

	This work	Referenced values		
GM	1.111(2)	1.118(3) [ref. 6]	1.115(3) [ref. 21]	---
MS-v2	1.111(2)	1.108(2) [ref. 4]	1.109(2) [ref. 21]	1.110(4) [ref. 23]
MS-v2r	1.112(2)	1.1121(8) [ref. 5]	---	---
VS	1.096(2)	1.101(6) [ref. 7]	1.099(2) [ref. 21]	1.10(3) [ref. 24]

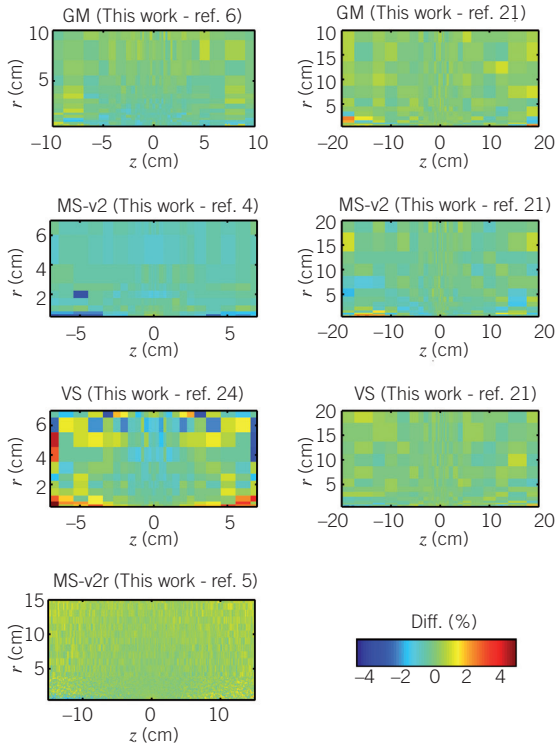

Fig. 4. Local difference in % of absorbed dose rate calculated in this work versus references. Each pixel corresponds to a point in the table of reference data being compared.

Table 3. Dose radial function obtained in this work for semi-infinite phantom.

r (cm)	GM	MS-v2	MS-v2r	VS
0.25	0.994(1)	0.993(1)	0.993(1)	0.992(1)
0.5	0.996(1)	0.999(1)	0.994(1)	0.997(1)
0.75	0.995(1)	0.996(1)	0.996(1)	1.002(1)
1	1.000(1)	1.000(2)	1.000(2)	1.000(2)
1.5	1.001(1)	1.002(2)	1.003(2)	1.004(2)
2	1.002(1)	1.005(2)	1.003(2)	1.011(2)
3	1.006(2)	1.004(2)	1.007(2)	1.010(2)
4	1.004(2)	1.008(2)	1.011(2)	1.014(2)
5	1.006(2)	1.003(2)	1.002(2)	1.014(2)
6	0.990(2)	0.994(2)	0.991(2)	1.008(2)
7	0.985(2)	0.987(2)	0.994(2)	0.993(2)
8	0.974(2)	0.975(3)	0.968(3)	0.982(3)
9	0.953(2)	0.960(3)	0.955(3)	0.966(3)
10	0.947(2)	0.941(3)	0.940(3)	0.949(3)
12	0.899(2)	0.897(3)	0.899(3)	0.905(3)
14	0.847(2)	0.852(3)	0.847(3)	0.854(3)
16	0.795(2)	0.794(3)	0.792(3)	0.809(3)
18	0.742(2)	0.743(3)	0.741(3)	0.747(3)
20	0.693(2)	0.682(3)	0.690(3)	0.688(3)
25	0.550(2)	0.546(3)	0.552(3)	0.556(3)
30	0.422(2)	0.420(3)	0.424(3)	0.423(3)

cell. The statistical uncertainty in the reference point ($r=1$ cm and $z=0$ cm) has been 0.1%.

Comparisons of the data obtained in this work to the absorbed dose to water in cylindrical coordinates with the bibliographic data have been performed.

Fig. 4 shows a map of differences of absorbed dose rate distribution for different sources. These comparisons have shown a good agreement between the obtained values by PENELOPE simulations and those obtained by Taylor et al[21] with EGSnrc, except for small differences in contact with the source and cable. The average value of the differences[**] has been –0.01% for GM source (range between –1.6% and 3.0%), 0.2% for MS-v2 source (range between –1.1% and 0.9%) and –0.14% for VS source (range between –2.7% and 1.7%). A comparison with published data from Granero et al[5] for MS-v2r new geometry has been made. The average difference was 0.2% (range between –2.3% and 2.7%). For the GM source results comparison with Ballester et al[6], a semi-infinite water phantom has been used and a good agreement has been found with a mean difference of –0.4% and range between –1.8% and 0.9%.

MS-v2 source (reference values from Daskalov et al[4]) and VS source (reference values from Casado et al[24]) comparisons have been made with the obtained results from 15 cm radius water phantom. Results of MS-v2 have shown small differences between –1.4% and 0.6% with –0.2% average. For VS source, the

[**] Points with radius smaller than 5 mm have been ignored.

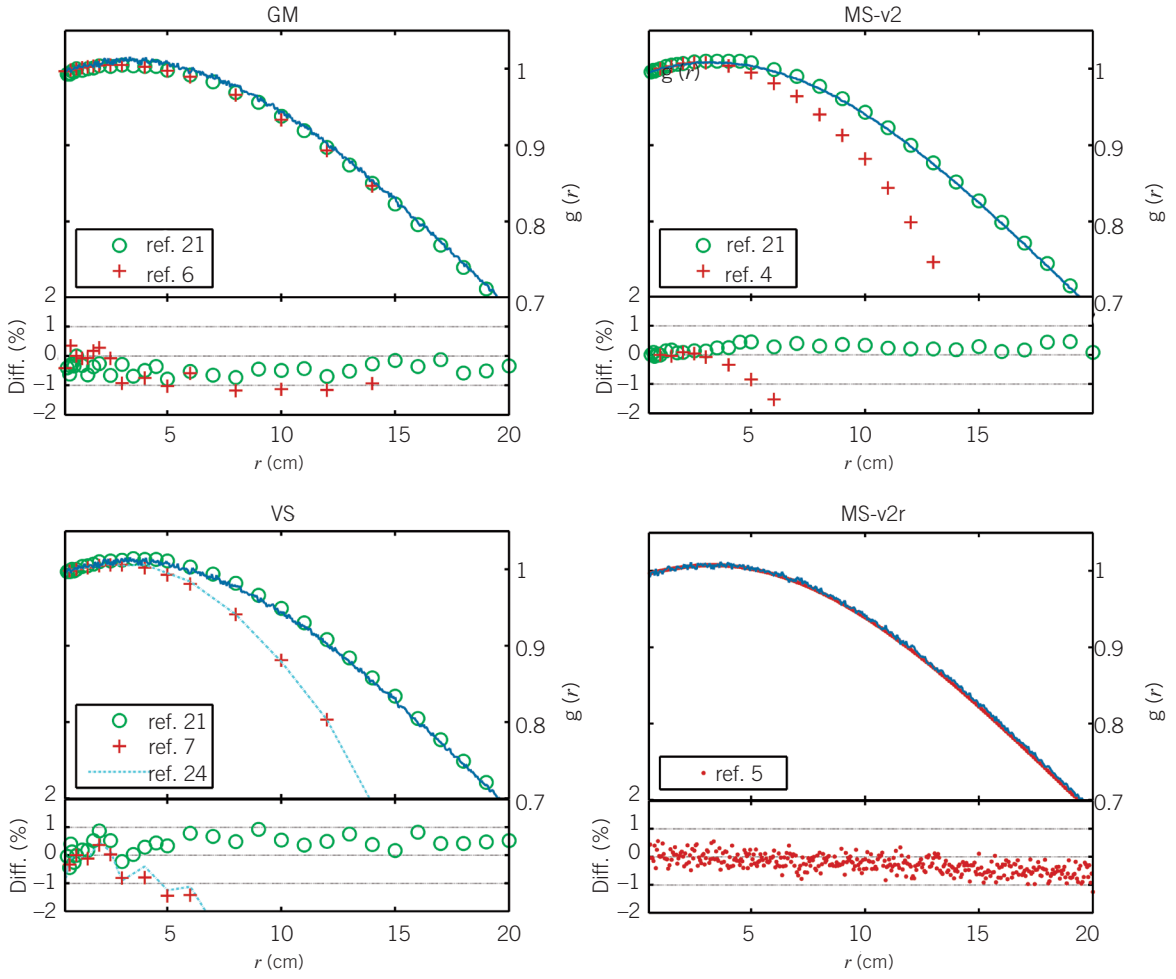

Fig. 5. Representation of the radial dose function and the differences in % for our results with semi-infinite phantom versus references.

differences are a little higher with –0.3% of average (range between –1.7% and 1.1%). The values tabulated in the reference with only two decimal places have been eliminated in the comparison.

TG-43 dosimetry parameters

TG-43 Parameters and functions have been calculated. A comparison of dose rate constants obtained in this work with PENELOPE with previous data is presented in table 2. MS-v2, MS-V2r and VS sources show a good agreement with the reference data, while GM source shows a significant difference if we consider the uncertainties of the results, although the difference is less than 1%. This difference may be due to the library of cross sections used in Geant3.21 (MC code used by Ballester et al[6]).

Table 3 shows the obtained values for the radial dose function through the discretization in cylindrical coordinates when the simulations are performed within a semi-infinite water phantom. A comparison*** of the radial dose function calculated in these conditions is presented in Fig. 5.

The radial dose function is the parameter that most clearly shows the influence of the phantom size in the calculations. It is observed that up to a radius of 5 cm, the differences are below 1%, but differences grow quickly from this value (2% to 6 cm, 4% to 8 cm and 7% to 10 cm). This question has already been discussed by other authors [23,27,28].

Results of radial dose function for 15 cm radius spherical water phantom have been shown in fig. 6 to validate our simulations for MS-v2 and VS source. These comparisons show very small differences (between –1% and 1%) for all sources.

*** Points with radius smaller than 5 mm have been ignored.

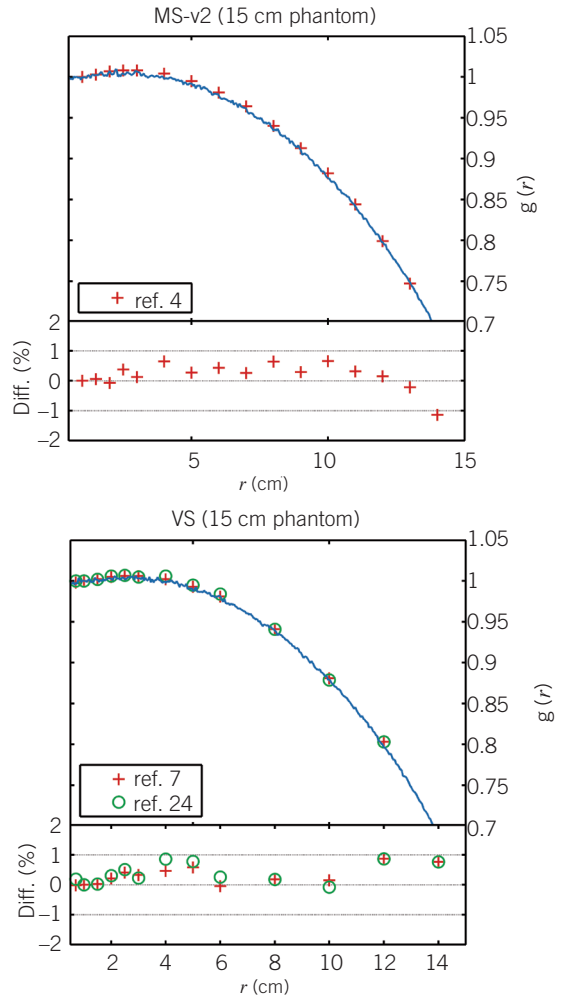

Fig. 6. Representation of the radial dose function and the differences in % for our results with 15 cm radius phantom versus references.

The dependence of dose radial function with phantom size shows the necessity to know the calculation conditions of the data entered in the planning system in order to determine the absorbed dose at radial distances greater than 5 cm (estimation of absorbed dose to distant organs or treatment implants in surface areas such as breast, cervix, etc.).

Some values of the anisotropy function are show in table 4 (calculated with spherical coordinate discretization). The agreement of the data obtained in this work with the data in references shows absolute differences below 2%. Moreover, anisotropy functions do not have significant phantom size dependence.

A complete set of results obtained in this work can be found at the link http://bqseeds.sarh.es. It presents 2D absorbed dose rate tables in water (along-away tables), dose rate constants, radial dose functions and anisotropy functions for the line source approach.

Table 4. Comparison of anisotropy function values obtained in spherical coordinates in some points. P-2008 indicates our results and "Ref's" shows results of ref. 6 for GM, ref. 4 for MS-v2, ref. 5 for MS-v2r and ref. 7 for VS. (*) Nearest value; (+) Interpolated value.

Angle	r(cm)	1				5				10				15			
	Source	GM	MS-v2	MS-v2r	VS	GM	MS-v2	MS-v2r	VS	GM	MS-v2	MS-v2r	VS	GM	MS-v2	MS-v2r	VS
30°	Ref. 22	0.902(2)	0.904(2)	---	0.940(2)	0.922(2)	0.919(1)	---	0.946(2)	0.933(2)	0.932(1)	---	0.953(2)	0.942(2)	0.940(1)	---	0.955(2)
	P-2008	0.915(2)	0.903(2)	0.909(2)	0.941(2)	0.921(2)	0.922(2)	0.923(2)	0.946(2)	0.933(2)	0.928(2)	0.942(2)	0.955(2)	0.939(2)	0.944(2)	0.950(2)	0.955(2)
	Ref's	0.912	0.9	0.911	0.94 (*)	0.927	0.91	0.926	0.94 (*)	0.939	---	0.938	0.95 (*)	0.945	---	0.944	0.95 (*)
60°	Ref. 22	0.980(2)	0.983(2)	---	0.991(2)	0.990(2)	0.984(1)	---	0.990(2)	0.990(2)	0.989(1)	---	0.991(2)	0.990(2)	0.988(1)	---	0.990(2)
	P-2008	0.989(2)	0.981(2)	0.983(2)	0.992(2)	0.987(2)	0.986(2)	0.982(2)	0.990(2)	0.987(2)	0.984(2)	0.990(2)	0.991(2)	0.984(2)	0.989(2)	0.993(2)	0.990(2)
	Ref's	0.985	0.98 (*)	0.985	0.99 (+)	0.989	0.98 (*)	0.987	0.99 (+)	0.988	---	0.989	0.99 (+)	0.988	---	0.989	0.99 (+)
120°	Ref. 22	0.983(2)	0.987(2)	---	0.996(2)	0.988(2)	0.980(1)	---	0.990(2)	0.989(2)	0.987(1)	---	0.993(2)	0.990(2)	0.986(1)	---	0.990(2)
	P-2008	0.987(2)	0.981(2)	0.987(2)	0.993(2)	0.985(2)	0.983(2)	0.986(2)	0.990(2)	0.988(2)	0.985(2)	0.989(2)	0.992(2)	0.985(2)	0.989(2)	0.993(2)	0.988(2)
	Ref's	0.985	0.91 (*)	0.985	0.99 (+)	0.988	0.93 (*)	0.987	0.99 (+)	0.989	---	0.989	0.99 (+)	0.989	---	0.989	0.99 (+)
150°	Ref. 22	0.906(2)	0.903(2)	---	0.941(2)	0.923(2)	0.915(1)	---	0.945(2)	0.936(2)	0.930(1)	---	0.954(1)	0.943(2)	0.939(1)	---	0.954(1)
	P-2008	0.913(2)	0.899(2)	0.908(2)	0.944(2)	0.924(2)	0.917(2)	0.926(2)	0.944(2)	0.934(2)	0.926(2)	0.935(2)	0.953(2)	0.933(2)	0.942(2)	0.947(2)	0.953(2)
	Ref's	0.914	0.90 (+)	0.910	0.95 (*)	0.93	0.92 (+)	0.924	0.95 (*)	0.94	---	0.936	0.95 (*)	0.94	---	0.942	0.95 (*)

Conclusions

MC simulations following current guidelines have been performed to get the full dosimetric characterization for the ^{192}Ir sources most widely used in Spain using the PENELOPE simulation code version 2008.1. The angular dependence of the intensity of air kerma for this type of sources as well as the differences in this value among the four sources considered have been shown.

The absorbed dose rate in water, the radial dose function and anisotropy function have been calculated. The results obtained are in good agreement with published data, also obtained with MC simulations, the differences between them can be explained by the difference in the interaction and transport models that implement different simulation codes, as well as small differences in the geometric description of the sources. The results were obtained with higher spatial resolution, lower statistical uncertainty and greater range than most of the published data. On the other hand, the simulations and calculations were performed using the same methodology for the four sources, which has been described in detail in this article. This facilitates the intercomparison of the results obtained from different sources, providing a compact set of dosimetric data obtained with PENELOPE 2008.1 for the ^{192}Ir sources most used in Spain.

The agreement between all the results obtained in this work with PENELOPE and the results from Taylor et al[21] obtained with EGSnrc is excellent. With the rest of references, due to different phantom sizes, results cannot be compared with the primary data obtained in this work and we have made simulations with finite size phantoms to compare with.

Acknowledgments

This work has been partially supported by the Spanish "Ministerio de Ciencia e Innovacion" under contract nos. FPA2009-14091-C02-02.

References

1. Nath R, Anderson L, Luxton G, Weaver K, Williamson J and Meigooni A Dosimetry of interstitial brachytherapy sources: Recommendations of the AAPM Radiation Therapy Committee Task Group No. 43, Med Phys 1995;22:209-34.
2. Rivard M, Coursey B, DeWerd L, Hanson W, Saiful Huq M, Ibbott G, Mitch M, Nath R and Williamson J, Update of AAPM Task Group No. 43 Report: A revised AAPM protocol for brachytherapy dose calculations, Med Phys 2004;31:633-74.
3. Li Z, Das R, DeWerd L, Ibbott G, Meigooni A, Pérez-Calatayud J,Rivard M, Sloboda R and Williamson J, Dosimetric prerequisites for routine clinical use of photon emitting brachytherapy sources with average energy higher than 50 keV, Med Phys 2007;34:37-40.
4. Daskalov G, Löffler E and Williamson J, Monte-Carlo aided dosimetry of a new high dose-rate brachytherapy source, Med Phys 1998;25:2200-2208.
5. Granero D, Vijande J, Ballester F and Rivard M, Dosimetry revisited for the HDR ^{192}Ir brachytherapy source model mHDR-v2, Med Phys 2011;38:487-94.
6. Ballester F, Puchades V, Lluch J, Serrano-Andrés M, Limami Y, Pérez Calatayud J and Casal E, Technical note: Monte-Carlo dosimetry of the HDR 12i and Plus ^{192}Ir sources, Med Phys 2001;28:2586-91.
7. Angelopoulos A, Baras P, Sakelliou L, Karaiskos P and Sandilos P, Monte Carlo dosimetry of a new ^{192}Ir high dose rate brachytherapy source, Med Phys 2000;27:2521-2527.
8. http://www.stal.com.cn/e_technicaldata.asp.
9. Chu S, Ekström L and Firestone R, The Lund/LBNL Nuclear Data Search, Version2.0, Feb 1999, available from http://nucleardata.nuclear.lu.se/NuclearData/toi/
10. Borg J and Rogers D W O, Monte Carlo calculations of photon spectra in air from Ir-192 sources, NRC Report PIRS-629R, 1998.
11. Salvat F, Fernández-Varea J M and Sempau J, PENELOPE-2008: A code system for Monte Carlo simulation of electron and photon transport, Workshop Proceedings, Barcelona, Spain. ISBN 978-92-64-99066-1.
12. Born M, Atomic Physics. Blackie and Son, London.
13. Hubbell J, Veigele W, Briggs E, Brown R, Cromet D and Howerton R, Atomic form factors, incoherent scattering functions, and photon scattering cross sections. J Phys Chem Ref Data 1975;4:471-538.
14. Cullen D, Hubbell J and Kissel L, EPDL97 The evaluated photon data library,'97 version, Report UCRL-50400 vol.6, rev.4, parts A and B (Livermore,CA: Lawrence Livermore National Laboratory).
15. Ribberfors R, X-ray incoherent scattering total cross sections and energy-absorption cross sections by means of simple calculation routines. Phys Rev A 1983;27:3061-70.
16. Berger M and Hubbell J, XCOM:Photon Cross Sections on a Personal Computer, Report NBSIR 87-3597 (Gaithesburg,MD: NIST) ,1987.
17. ICRU (1998). Fundamental Quantities and Units for Ionising Radiation. Report No. 60, International Commission on Radiation Units and Measurements, 7910 Woodmont Ave., Bethesda, Maryland 20814.
18. Higgins P, Attix F, Hubbell J, Seltzer S, Berger M and Sibata C, Mass Energy-Transfer and Mass Energy-Absorption coefficients, including in-flight positron annihilation for photon energies 1 keV to 100 MeV. NISTIR 4680, National Institute of Standars and Technology, Gaithersburg, MD (1991).
19. Hubbell J and Seltzer S, Tables of X-Ray Mass Attenuation Coefficients and Mass Energy-Absorption Coefficients (version 1.03). http://physics.nist.gov/xaamdi [2004]. NIST, Gaithersburg, MD.
20. Taylor R and Rogers D W O, An EGSnrc Monte Carlo-calculated database of TG-43 parameters, Med Phys, 2008;35,4228-4241.
21. Taylor R and Rogers D W O, EGSnrc Monte Carlo calculated dosimetry parameters for ^{192}Ir and ^{169}Yb brachytherapy sources, Med Phys 2008;35:4933-4944.

22. Lis Boada M, Ballester Pallarés F and Pérez Calatayud J, Parámetros Dosimétricos de fuentes de Cs-137 e Ir-192 en Braquiterapia, http://www.uv.es/braphyqs.

23. Berenguer Serrano R, Rivera Giménez M, Núñez Quintanilla A and Gutiérrez Pérez M, Evaluación de la dosimetría de una fuente de Ir-192 de alta tasa en un medio con dispersión incompleta mediante cálculo de Monte Carlo, Revista de Física Médica 2006;7(3):107-112.

24. Casado F, García-Pareja S, Cenizo E, Mateo B, Bodineau C and Galán P, Dosimetric characterization of an ^{192}Ir brachytherapy source with the Monte Carlo code PENELOPE, Phys Med, 2010;26(3):132-139.

25. Evaluation of measurement data - Guide to the expression of uncertainty in measurement, International Organization for Standardization (ISO). Joint Committee for Guides in Metrology (JCGM 100, 2008). Corrected version 2010. http:\\www.bipm.org/utils/common/documents/jcgm/JCGM_100_2008_E.pdf

26. DeWerd L, Ibbott G, Meigooni A, Mitch M, Rivard M, Stump K, Thomadsen B and Venselaar J, A dosimetric uncertainty analysis for photon-emitting brachytherapy sources: report of AAPM Task Group No. 138 and GEC-ESTRO. Med Phys, 2011;38:782-801.

27. Pérez-Calatayud J, Granero D and Ballester F, Phantom size in brachytherapy source dosimetric studies, Med Phys 2004;31:2075-81

28. Melhus C and Rivard M, Approaches to calculating AAPM TG-43 brachytherapy dosimetry parameters for ^{137}Cs, ^{125}I, ^{192}Ir, ^{103}Pd, and ^{169}Yb sources, Med Phys 2006;33:1729-37